ACS OMEGA

http://pubs.acs.org/journal/acsodf

Article

Imparting Fire Retardancy and Smoke Suppression to Leather during Tanning Processes

Guadalupe Sanchez Olivares,* Alexander Battig, Sebastian M. Goller, Daniel Rockel, Victor Ramírez González, and Bernhard Schartel*

Cite This: *ACS Omega* 2022, 7, 44156−44169

Read Online

ACCESS | Metrics & More | Article Recommendations | Supporting Information

ABSTRACT: Leather is considered a luxury good when used in seating and upholstery. To improve safety, flame retardancy in leather is usually achieved through various finishing processes such as spray or roller coating. These treatments require processing steps that cost time and are labor-intensive. One avenue to achieving flame retardancy in leather is to add flame retardants during the tanning process. However, the influence on flame retardancy exerted by specific intumescent additives specifically added during leather tanning has yet to be investigated. This work explores the roles played by intumescent additive compounds in flame retarding leather when they are added during tanning instead of applied as a coating. Via a systematic investigation of various compound mixtures, the flame retardant effects in the condensed and the gas phases are elucidated. The results show a strong impact of melamine in the gas phase and of polyphosphates in the condensed phase. Their impact was quantified in fire and smoke analysis, showing a 14% reduction in the peak of heat release rate, strongly reduced burning lengths, and a 20% reduction in total smoke release compared to nontreated leather. These results illuminate the key role played by specific compounds in the flame retardancy of leather, particularly when they are added specifically during the tanning process instead of being applied as a coating. This method has great potential to reduce processing steps, lower costs, and improve material safety.

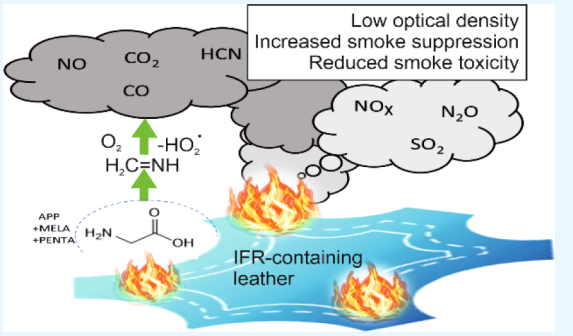

1. INTRODUCTION

Currently, the leather industry plays a prominent role in the world economy with an estimated global trade value of approximately US $100 billion per year.[1] Leather is considered a luxury good, and consumer demands on this material are high, which has fueled research into creating cleaner and safer leather.[2] Leather is often utilized in upholstery material and for furniture and seats in the transport industry. Consequently, leather must fulfill specifications for flammability. The density and toxicity of smoke generated in fires are a major concern. Upholstered seat materials are generally quite combustible and may smolder in the presence of a small ignition source.[3]

In the tannery industry, fire protection features of leather are commonly achieved through a finishing process,[4] most often accomplished by applying a coating to the leather surface by spraying, roller coating, or a pad-dry cure method using products containing flame retardant (FR) additives.[5] However, new strategies to impart fire protection characteristics to leather during retanning,[6] fatliquoring,[7] and dyeing processes have been considered. These have focused mainly on the addition of nanoparticles, which may become incorporated into leather fibers.[8] This is achieved by either physical adhesion or grafting to leather fibers by chemical bonding in order to reduce the number of FR finishing steps for leather to be used in upholstery applications.

The effect of sodium montmorillonite content on the FR and mechanical properties of semifinished leather has been investigated. Clay mineral particles added after the retanning processes as a dispersion in water were homogeneously dispersed into the internal structure of the leather. This significantly reduces the burning lengths of semifinished leather in flammability tests as a consequence of barrier formation during combustion promoted by the presence of clay particles. Tensile and tear strength were also improved at specific filler contents.[9] Combinations of additives containing layered double hydroxide have also been investigated[10] to reduce leather flammability. A graphene oxide-grafted maleic anhydride vinyl acetate copolymer has been used as a retanning agent for leather: graphene oxide acts to modify collagen fibers, and this hybrid penetrated collagen fibers. For combustion under forced flaming conditions, the key values for the peak of heat release rate (−11%), carbon monoxide production (−29%), and total smoke production (−11%) were

Received: August 31, 2022
Accepted: November 9, 2022
Published: November 22, 2022

https://doi.org/10.1021/acsomega.2c05633
ACS Omega 2022, 7, 44156−44169

reduced for retanned leather. During the combustion of a copolymer containing 2 wt % graphene oxide, a barrier was formed as a consequence of the presence of graphene oxide sheets in the collagen fibers.[11] Similar observations have been reported for chrome tanning.[12] Furthermore, organic layered double hydroxides (O-LDHs) have been used in conjunction with seed oil during leather fat liquoring processes to reduce flammability. Most notably, there was a reduction in the after-flame time, length of charring, and smoke density during flame testing. The O-LDH particles became well dispersed during fat liquoring, forming an inorganic−organic network with collagen fibers and acting to promote the formation of a physical barrier in fires.[13] Similar effects on flammability, attributed mainly to barrier formation during the combustion of leather, have been noted for treatment with nanofat liquors.[14]

Intumescent flame retardant (IFR) mixtures are often applied to the surface of fibrous materials in order to reduce flammability. However, the integration of these materials into the fabric improves flame retardancy.[15] Phosphorus and nitrogen-based IFRs have been investigated for use with leather: *tetrakis*-hydroxymethyl phosphonium-melamine phosphate salt (THPMP) was synthesized and applied during the tanning processes for pigskin.[16] The thermal decomposition kinetics and flammability of wet blue leather containing THPMP have been investigated. A three-step kinetic decomposition was implemented, first of triglyceride, then multicomplexed collagen, and finally singly complexed collagen for leather during pyrolysis. Crosslinks were formed.[17] Melamine's role in flame retardancy and smoke suppression during the combustion of polar cross-linked polymers has been investigated. The evolution of decomposition products from the condensed phase dilutes the fuel load in the combustion zones.[18]

In an innovative approach to flame retardancy for leather, the performance of IFR additives added specifically during tanning processes has been investigated for their ability to impart fire protection features in semifinished bovine leather (crust leather). An improvement in flame retardancy and smoke suppression in fire scenarios has been sought. To understand which components might facilitate high flame retardancy, the flammability of unfilled leather has been compared to that of leather containing a single component (melamine, pentaerythritol, and ammonium polyphosphate), containing a combination of two components, and containing combinations of three components. The interaction of each component and their various combinations as an additive to leather is analyzed to determine whether IFR additives may afford FR properties to leather after tanning. This method of imparting flame retardancy to leather yields great potential in improving safety and especially lowering processing costs of this distinctive material, as intumescent compounds are widely available. This work aims to outline, as a proof of principle, how commercially available FRs may be implemented in a unique processing method to improve flame retardancy and smoke suppression, and how particular components affect the fire performance of the proteinaceous leather matrix.

2. MATERIALS AND METHODS

Pieces of bovine wet blue leather (12 kg, thickness = 1.1−1.4 mm) were supplied by a local tannery industry in Mexico. Trivalent chromium sulfate of 42% basicity, synthetic and vegetal retanning agents, formic and phosphoric acids, surfactant agents, sodium formate, as well as sulfinated natural and synthetic fatting products (industrial grade) were purchased from local suppliers (León, Gto., Mexico). Ammonium polyphosphate Exolit AP422 (APP) was supplied by Clariant GmbH (Wiesbaden, Germany); the phosphorus content was between 31 and 32 wt %, and the material had an average particle size D50 of 17 microns. The purity of melamine (MELA) was 99.8% and that of pentaerythritol (PENTA) was between 94 and 95%; both were purchased from ABAQUIM, S.A. de C.V. (Mexico City, Mexico).

See the Supporting Information for additional characterization methods.

Flame-retarded semifinished leather (crust leather) was obtained by conventional retanning, dyeing, fat liquoring, and drying processes[19,20] using type CR10/1 tannery testing drums from Italprogetti (Italprogetti SpA, San Romano, Italy). The drums were 1.0 m in diameter and 0.50 m in width and ran at a rotational speed of 16−18 rpm. The added mass in weight percent (wt %) of IFR additives, chemicals, or auxiliary products was based on the mass of the piece of wet blue leather (Table 1).

Table 1. Sample Identification Code of Investigated Leather Samples and Loading of IFR Additives Aluminum Polyphosphate (APP), Melamine (MELA), and Pentaerythritol (PENTA) in IFR Leather Specimens

sample identification	APP/wt %	MELA/wt %	PENTA/wt %
leather			
APP_12	12		
MELA_12		12	
PENTA_12			12
MELA_6/PENTA_6		6	6
APP_6/MELA_6	6	6	
APP_6/PENTA_6	6		6
INTUM_3	1	1	1
INTUM_6	2	2	2
INTUM_12	4	4	4

The retanning, dyeing, fat liquoring, and drying processes were performed as follows:

1. Washing: 200 wt % water at 40 ± 5 °C to standardize wet blue leather quality using 0.2 wt % surfactant agent. The pH was maintained at 3.3−3.8 using formic acid for the leather sample without FR additives and phosphoric acid for leather samples with FR additives. Rotating time: 20 min.
2. Draining.
3. Pre-retanning: 100 wt % water at 40 ± 5 °C and 3 wt % trivalent chromium sulfate. Rotating time: 40 min.
4. Neutralization: 0.8 wt % sodium formate; the desired pH value was reached at 4.5−5.0. Rotating time: 40 min (approximately).
5. Draining.
6. Washing: 200 wt % water at room temperature. Rotating time: 10 min.
7. Draining.
8. Retanning: 50 wt % water at room temperature, 2 wt % synthetic and vegetal retanning agents. Rotating time: 60 min.
9. Addition of FR additives: additive amount according to Table 1. Rotating time: 40 min.
10. Dyeing: 3 wt % aniline. Rotating time: 40 min.

https://doi.org/10.1021/acsomega.2c05633
ACS Omega 2022, 7, 44156−44169

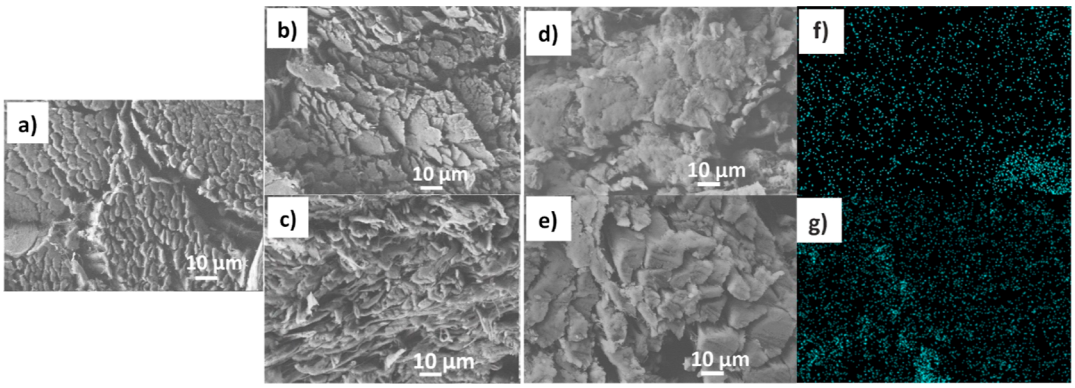

Figure 1. SEM micrographs of cross sections of (a) leather, (b) MELA_12, (c) MELA_6/PENTA_6, (d) APP 6_MELA_6, and (e) INTUM_6 samples and phosphorus elemental mapping of APP_6/MELA_6 (f) and INTUM_6 (g) samples.

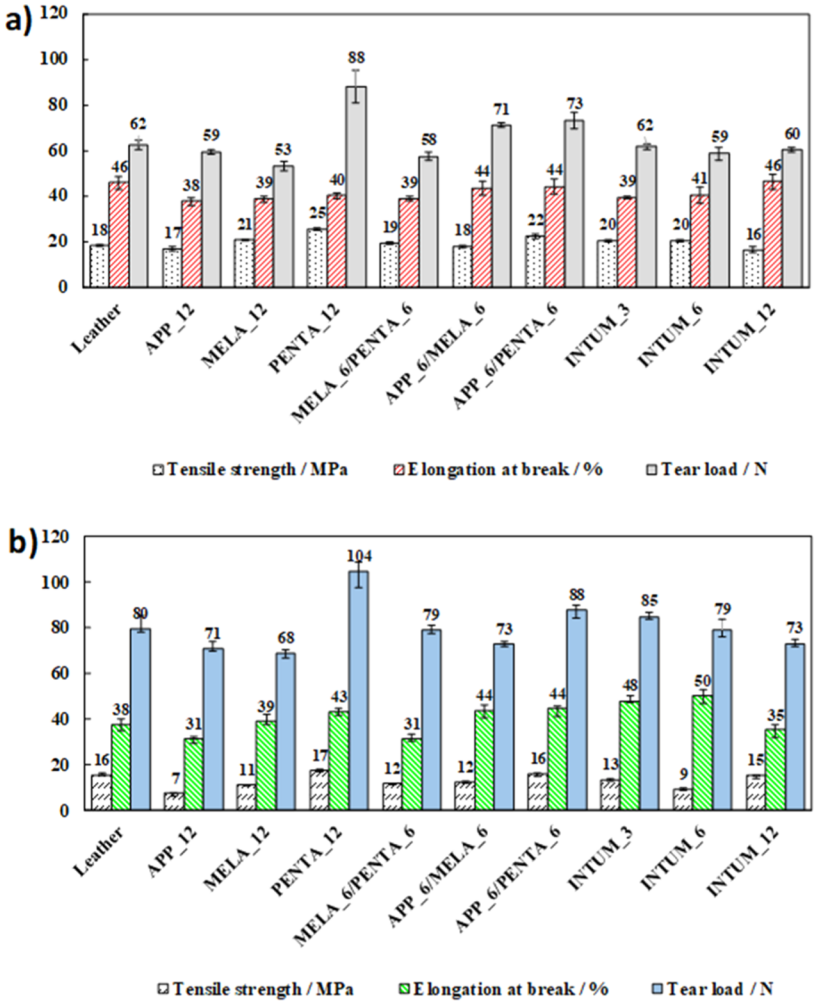

Figure 2. Tensile strength, elongation at break, and tear load parallel (a) and perpendicular (b) to the backbone of investigated leather samples.

11. Fat liquoring: 100 wt % water at 50 °C, 4 wt % sulfited natural and synthetic fatting products. The pH was reduced to values between 3.3 and 3.8 formic or phosphoric acid. Rotating time: 45 min.
12. Draining.
13. Washing: 150 wt % water at room temperature. Rotating time: 10 min.
14. Draining.
15. Drying: semifinished leather was dried under vacuum to obtain 14−15% humidity.

The investigated specimens are identified by their filler content and IFR additive type. Table 1 displays the composition and sample IDs of specimens investigated herein. Unfilled leather is compared to leather containing 12 wt % of one IFR compound (MELA, APP, or PENTA), 6 wt % of one compound, and 6 wt % of another IFR compound (MELA/PENTA, APP/MELA, or APP/PENTA), and finally, equal

https://doi.org/10.1021/acsomega.2c05633
ACS Omega 2022, 7, 44156−44169

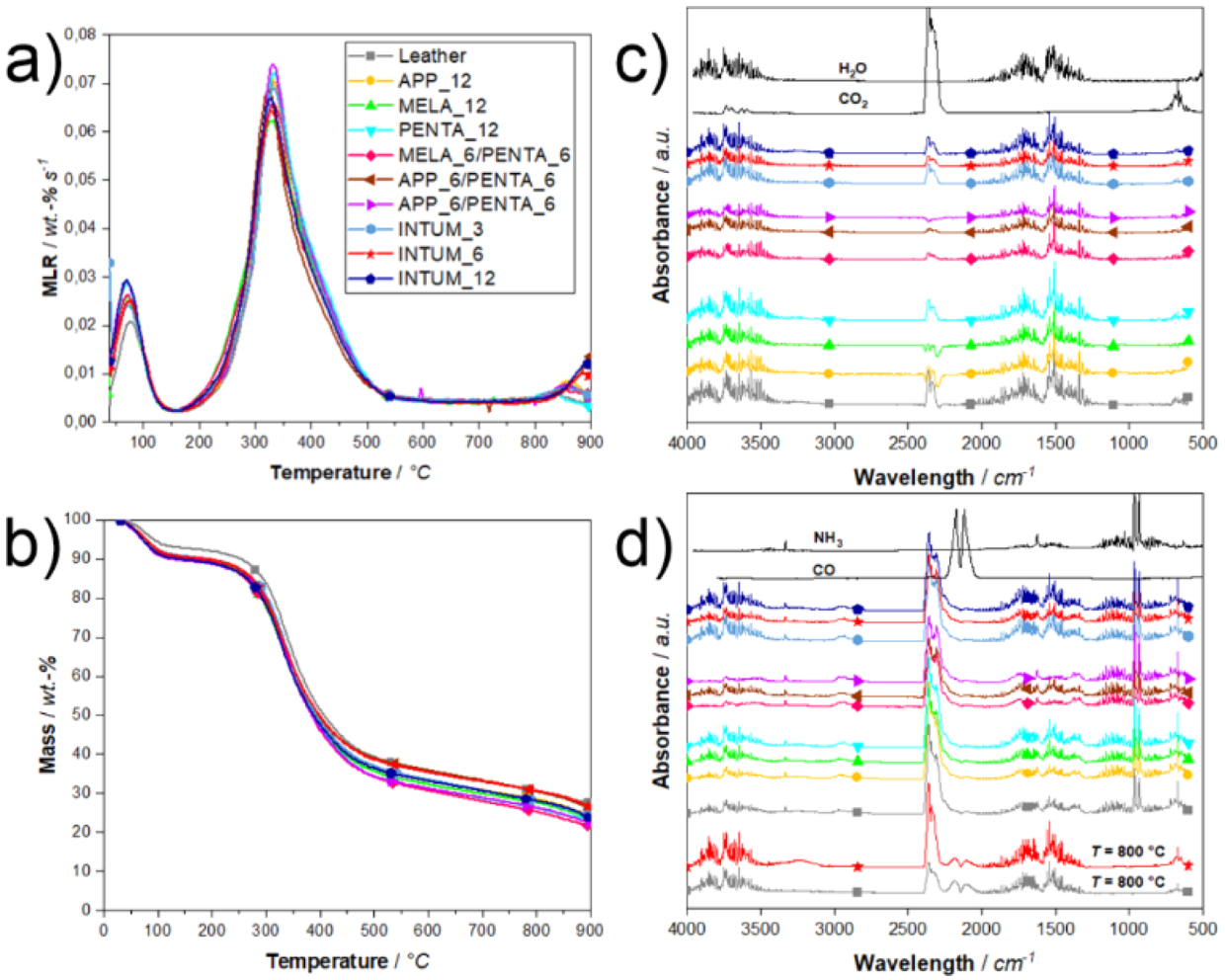

Figure 3. (a) MLR and (b) mass loss as a function of temperature from TGA; (c) IR spectrum at the first decomposition step (T_1); (d) IR spectrum at the main decomposition step (T_{max}) and at 800 °C for unfilled leather and INTUM_6.

parts of all three components at 3, 6, and 12 wt % loadings (INTUM).

3. RESULTS AND DISCUSSION

3.1. Morphology. The surface morphology of leather samples was investigated to understand how specific additives affect the material properties. Scanning electron microscopy (SEM) revealed changes in the morphology of leather samples depending on the filler type. Figure 1 displays the micrographs of cross sections of unfilled leather and MELA_12, MELA_6/PENTA_6, APP_6/MELA_6, and INTUM_6 samples. In Figure 1a, unfilled leather displays a fine fiber network structure (d = 3−6 μm). At the fiber bundle level, interfiber spaces were visible. The IFR samples MELA_12, MELA_6/PENTA_6, APP 6_MELA_6, and INTUM_6 exhibited a noticeably altered fiber network morphology (Figure 1b−e). These samples showed better filling, and the network of fibers was more compact. The fibers appeared agglutinated, forming layers to some extent (not well-defined interfiber spaces). The altered morphology was attributed to the penetration of IFR additives through leather pores via mechanical action (friction, compression/release movement, and turbulent flow of the float due to speed and drum).

Deriving from phosphorus elemental analysis, the IFR particles were well deposited among the fibers. The distribution and dispersion of APP (APP_6/MELA_6 and INTUM_6) were investigated by phosphorus elemental analysis (SEM−EDX) (Figure 1f,g). Both samples display fine dispersion and distribution of phosphorus, indicating APP within the three-dimensional structure of leather. The distribution of APP throughout the sample is relevant to the flame retardancy of leather. In fire scenarios, the phosphorus and nitrogen compounds may interact with collagen to form residues and lower fire loads.

3.2. Mechanical Properties. The mechanical properties of leather depend mainly upon the structure of the fibers throughout the corium. The final fiber network structure is affected by tanning processes, and several variables influence its 3D structure, such as the amount of crosslinking, the angle of fiber weave linking, the number of fibers, their separation/apparent density, the tanning agent and drying process used, water content, the age, breed, sex, diet, and husbandry of the animal, the storage history, etc.[19,21] To evaluate the mechanical properties of IFR leather (Figure 2) parallel (Figure 2a) and perpendicular (Figure 2b) to the backbone, tensile strength, elongation at break, and tear load were determined. These measurements help highlight the impact of IFR compounds on material properties and durability during leather tanning.

Leather samples displayed better tensile strength in the parallel than in the perpendicular direction. This observation is consistent with stress distribution throughout the fiber

https://doi.org/10.1021/acsomega.2c05633
ACS Omega 2022, 7, 44156−44169

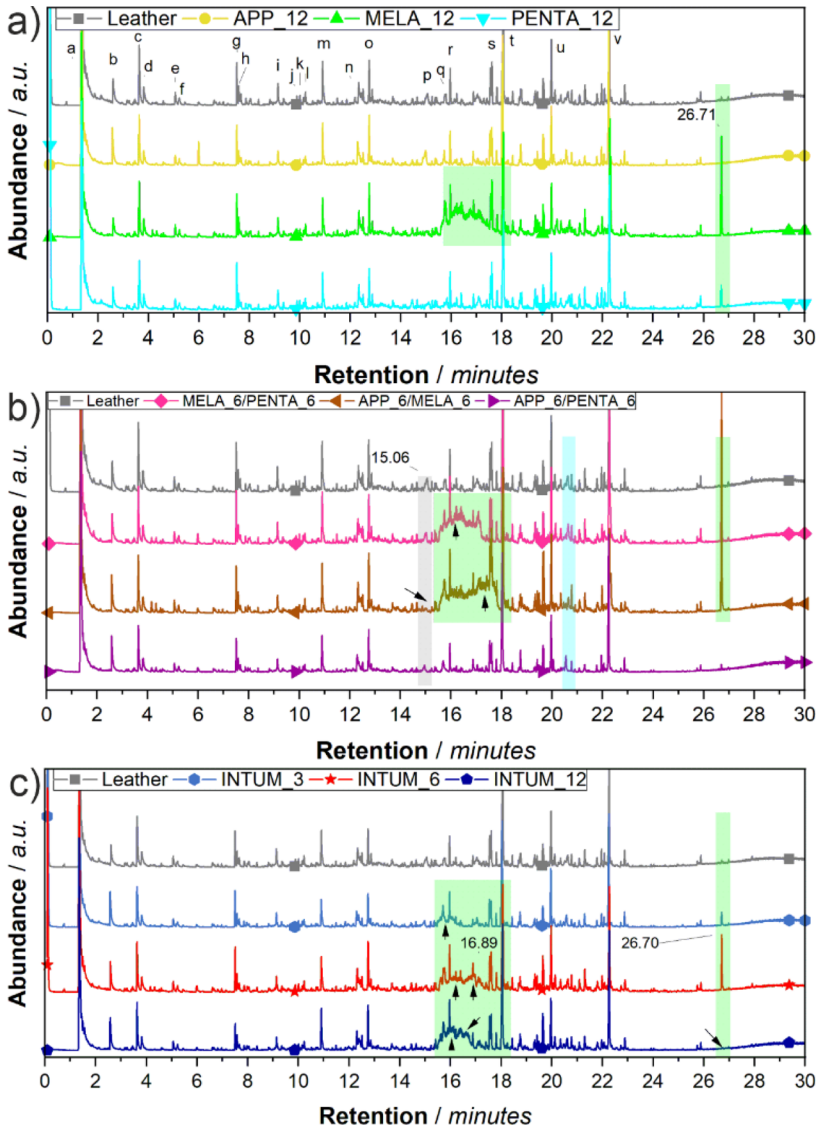

Figure 4. Gas chromatograms of leather with various fillers via Py-GC/MS (T = 500 °C); (a) single components at 12 wt % loading, (b) two components at 6 + 6 wt %, and (c) IFR mixtures at 3, 6, and 12 wt % loading.

networks, which are oriented parallel to the test direction. The tear load was higher in samples in the perpendicular direction, and this phenomenon was attributed to the crosslinking and linking of fibers throughout the corium structure. When weave fibers are angled opposite to the test direction, more force is required to split up and break fibers. Among the IFR leather samples with a single filler, PENTA_12 displayed the highest tear load in both directions to the backbone (80 N parallel and 104 N perpendicular), indicating an impact on tear resistance. Among two-filler IFR leathers, APP_6/MELA_6 and APP_6/PENTA_6 displayed a higher elongation at break and tear load than unfilled leather in both directions to the backbone. This indicates a fortifying effect of APP in combination with PENTA or MELA. For INTUM_3, INTUM_6, and INTUM_12, while the mechanical properties in the parallel direction decreased slightly with increasing IFR additive contents compared to unfilled leather, the tensile strength was slightly reduced for INTUM_12.

Thus, the results show that the tensile strength, elongation at break, and tear load of IFR samples depend on the type, combination, and content of additives. Various filling effects, such as the deposition, dispersion, and distribution of IFR particles among fibers, contribute to the mechanical properties. The additives produced a lax fiber matrix structure with separations between fibers or fiber bundles. The mechanical properties changed with fiber laxity, and more "loose" fibers produced soft and flexible leather. Increased fiber separation allowed free movement of the fibers, resulting in relatively good tensile strength, elongation at break, and tear load. However, excessive fiber laxity resulted in low tensile strength and tear load but high elongation at break. A limited laxity produces rigid leather, which points to a highly compact structure.[22] In this regard, INTUM_12 presented a higher elongation at break, yet low tensile strength compared to INTUM_3 and INTUM_6. This result provides evidence for a reinforcing effect of the IFR compounds when all are combined at an optimal content. Moreover, PENTA_12 displayed higher tear load and tensile strength than APP_12 and MELA_12. This result was attributed to a compact structure, yet the notable increment in tear load for PENTA_12 may be attributed to the intrinsic mechanical properties of that specific leather sample.[23]

https://doi.org/10.1021/acsomega.2c05633
ACS Omega 2022, 7, 44156−44169

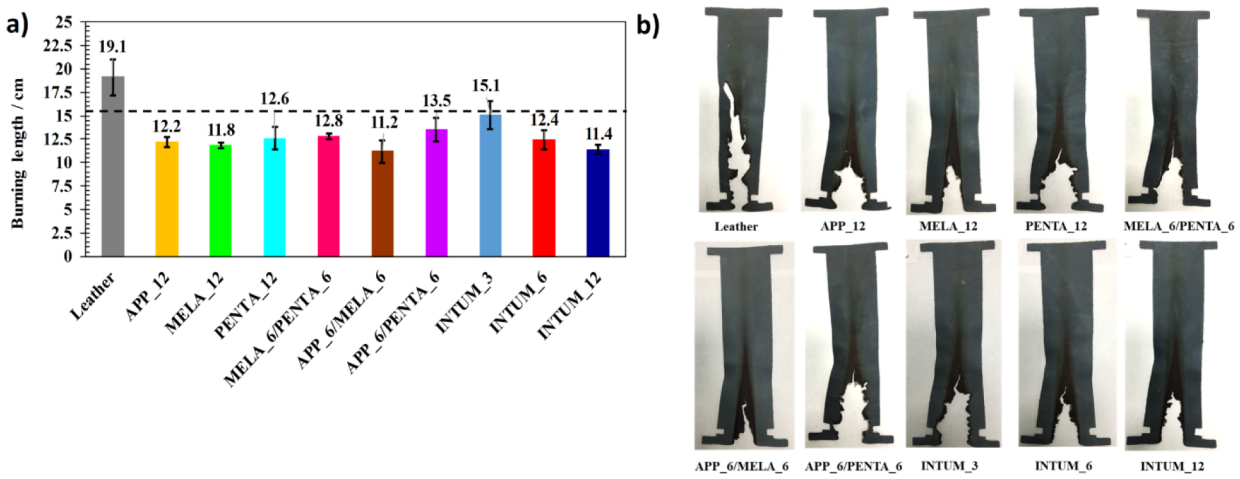

Figure 5. Burning length of unfilled leather and IFR-containing samples (a); the dashed line indicates a 15.2 cm maximum value of burning length according to the vertical flammability test 14 C.F.R. Appendix F to Part 25 Part I, criteria (a) (1) (i). Digital images of evaluated specimens (b).

3.3. Pyrolysis. *3.3.1. Thermogravimetric Analysis and Evolved Gas Analysis (TG-FTIR).* To understand the effect on pyrolytic decomposition, unfilled leather and IFR leather samples were investigated via thermogravimetric analysis (TGA) (Table S1). Figure 3a displays the mass loss and Figure 3b the mass loss rate (MLR) as a function of temperature. The curves display mass loss immediately upon heating, which was attributed to water (Figure 3b). Leather samples retained varying degrees of water, about 8−10 wt %. All materials showed two decomposition steps, and the first decomposition step (T_1) was between 71 and 76 °C. The onset temperature (onset T_{max}) (152−166 °C) marked the beginning of the main decomposition step, and the T_{max} was between 325 and 334 °C (mass loss: 55−58 wt %). Evolved gases from pyrolysis were analyzed by TG-FTIR, and Figure 3c,d shows the FTIR spectra of the two decomposition steps and those at a mass loss above 800 °C.

The mass loss curves revealed some minor changes to the pyrolytic decomposition.

INTUM_6 achieved a slightly higher onset T_{max} compared to unfilled leather, as the IFR compounds improved the thermal stability of leather during pyrolysis. MELA_12 and PENTA_12 exhibited a slightly higher mass loss (58 wt %) than unfilled leather, which was attributed to the gasification of those compounds. Correspondingly, MELA_6/PENTA6 displayed a lower onset T_{max} (152 °C) and elevated mass loss (59 wt %) compared to the reference. APP_6/MELA_6, INTUM_6, and INTUM_12 showed lower mass loss (55−56 wt %), illustrating higher thermal stability for IFR leather specimens containing APP.

After the main decomposition step above 500 °C, the samples continued to lose mass with increasing temperature, indicating thermally unstable residues (Figure 3a). Leather formed a carbonaceous residue due to the charring of protein fibers. When IFR compounds were implemented during the tanning of leather, high residue yields were attained by APP_6/MELA_6 (32 wt %), a 28% increase compared to MELA_6/PENTA_6 and a 14% increase compared to unfilled leather. The absence of APP led to lower residues (MELA_12: 27 wt %; PENTA_12: 26 wt %; MELA_6/PENTA_6: 25 wt %). This phenomenon illustrates that APP played a prominent role in residue formation in IFR leather samples. At elevated temperatures, those residues containing APP were more temperature-stable above 500 °C due to the interaction of collagen with phosphorus in the condensed phase before and at T_{max}.

The FTIR spectra at T_1 (Figure 3c) revealed that mainly water (between 4000 and 3500 cm^{-1}) was formed. The spectra at T_{max} (Figure 3d) exhibited strong bands characteristic for water, carbon dioxide (2360 cm^{-1}), and ammonia (3330, 960, and 930 cm^{-1}), and also weaker bands for carbon monoxide (2180 and 2120 cm^{-1}). The bands below 3000 cm^{-1} point to aliphatic hydrocarbon compounds. Above 800 °C, CO was the main product in the FTIR spectra, along with aromatic signals above 3000 cm^{-1}. As collagen constitutes the structural protein of leather, polypeptides consisting of amino groups, aliphatic C−H chains, and hydroxylic and carboxylic groups decomposed into CO, CO_2, NH_3, and H_2O via hydrolysis and chain scission reactions. The measured spectra reflect the decomposition of proteinaceous compounds. Due to strong signals stemming from leather decomposition products, IFR compounds were largely indistinguishable in the gas phase via TG-FTIR analysis. Further gas-phase analysis was needed to understand the pyrolytic decomposition of leather which was tanned in combination with IFR compounds.

3.3.2. Pyrolysis−Gas Chromatography/Mass Spectrometry (PY-GC/MS). The chromatographs of unfilled leather and of IFR leather at various loadings (Figure 4) revealed that the thermal cracking products of leather at 500 °C via pyrolysis−gas chromatography/mass spectrometry showed decomposition products, which were characterized in detail. This data provided insight into the composition of the gaseous decomposition products of leather. Additional data are presented in the Supporting Information (Table S2 and Figures S1 and S2).

Table S2 shows that specific compounds (a−v) were identified in the gas phase. Ammonium carbamate was detected in relatively high abundance, and its occurrence is linked to the decomposition of glycine [retention time (RT) 1.36 min [peak a]]. Moreover, pyrrole (peak c, RT 3.64 min), aniline (peak g, RT 7.51 min), naphthalene (peak m, RT 10.91 min), 2-methylnaphthalene (peak o, RT 12.75), and more complex nitrogen-containing hydrocarbons like hexahydropyrrolo[1,2-A] pyrazine-1,4-dione (peak t, RT 18.07) and hexahydro-3-(2-ethylpropyl)-pyrrolo[1,2-A] pyrazine-1,4-dione were measured above 17 min. The latter two

https://doi.org/10.1021/acsomega.2c05633
ACS Omega 2022, 7, 44156−44169

compounds are products of cyclization reactions between glycine and proline (cyclo-(Gly-Pro)) and of leucine and proline (cyclo-(Leu-Pro)), respectively. These compounds, as well as DL-alanylglycylglycine dihydrate (peak q, RT 15.78 min), further point to hydrolytic scission and the gasification of peptide fragments along the polypeptide chain.

When IFR compounds were implemented in the tanning processes, changes to the material decomposition in the gas phase were noticeable. A broad signal between 15.6 and 18.2 min corresponding to melamine was detected, which was characteristic for the samples MELA_12, MELA_6/PENTA_6, and APP_6/MELA_6. This signal was clearly absent in APP_6/PENTA_6 (Figure 4a), the sample without melamine. The signal differed in shape from the broad signals for MELA_6/PENTA_6 and APP_6/MELA_6, and this behavior suggests changes in concentration caused by the interaction of MELA and APP upon decomposition. INTUM_6 exhibited higher abundancies between 16.0−17.5 min compared to other INTUM samples. The signal from bis(2-ethylhexyl) terephthalate at 26.7 min was particularly affected by melamine (Figure S2), likely caused by cyclization reactions occurring in the presence of melamine: its formation was most prominent in MELA_12, APP_6/MELA_6, and INTUM_3, pointing to melamine impacting the gas phase. Thus, the pyrolysis investigation revealed that melamine plays a key role in the gas phase during pyrolysis and that APP is key to the formation of complex phosphorus−nitrogen-rich compounds. The presence of these additives suggests that they remained robust throughout the tanning process.

3.4. Fire Testing. *3.4.1. Reaction to Small Flame.* Under rigorous flammability conditions, leather is a flammable material with a high tendency to smolder. However, natural leather is not highly flammable under common flammability test conditions. This phenomenon was highlighted in reaction-to-small-flame tests. Here, vertical flammability tests were performed by applying a flame of 38 mm length for a total of 60 s (Figure 5a), although the American Leather Chemist's Association Method E 50 "Fire resistance of leather"[24] indicates the application of a 38 mm flame for only 12 s.

When IFR additives were used in the tanning of leather, the tested samples displayed reduced burning lengths. Unfilled leather exhibited a 19.1 cm burning length, whereas all IFR samples remained below 15.2 cm (maximum value according to the test criteria). The melamine sample MELA_12 exhibited a shortened burning length (11.8 cm), and APP_6/MELA_6 produced the greatest reduction (−41%) in burning length to 11.2 cm. This phenomenon points to an interaction of APP and MELA in INTUM samples, which exhibited a tendency to reduce burning lengths with increasing IFR content. Figure 5b shows digital images of specimens subjected to the vertical flammability test. The burned areas were clearly distinguishable, and the burning length of unfilled leather was clearly the greatest among all specimens.

Leather is a natural polyamide chemically modified by tanning agents, oils, and finishing components. It burns slowly via glowing (smoldering), usually emitting smoke. Mineral tanning agents, especially chromium salts, induce afterglow through the catalytic oxidation of carbon.[24] Table S3 discloses afterglow times from the vertical flammability test. Here, unfilled leather showed the longest afterglow time (51 min), while APP_6/MELA_6 showed a 2 min afterglow time, which was a 96% reduction compared to unfilled leather.

These results highlight the effect IFR additives, particularly melamine, have on reducing burning lengths and lowering afterglow time. Melamine's FR mode of action consists in diluting the flame zone and cooling due to high endothermic decomposition. Moreover, noncombustible gases (CO_2, water vapor, and NH_3) are released.[25] Melamine acts as a blowing agent and char promoter in the condensed phase,[26] accompanied by ammonium polyphosphate and pentaerythritol.[27] The char layer forms a physical barrier, slowing down heat and mass transfer between the gas and condensed phases during a fire.[6,28]

3.4.2. Forced Flaming Behavior. The forced flaming behavior of IFR leather was determined using a cone calorimeter (Table 2). Figure 6 displays the results from unfilled leather compared to IFR leathers, where the heat release rate (HRR), total heat released (THR), and total smoke release (TSR) are displayed as functions of time. All leather samples (thickness = 1.4 mm) exhibited a time to ignition (t_{ig}) of 32−38 s at an irradiation of 50 kW m^{-2}. This result highlights the inherently low flammability of leather. Unfilled leather exhibited extended smoldering prior to ignition, and high smoke production was observed. The HRR curves indicate that the materials were thermally thin.[29] Unfilled leather burned for 70 s, and the burning times were largely unchanged for IFR leathers. Specimens continued to thermally oxidize after flameout, as illustrated by the increasing THR in Figure 6b above 120 s (flameout). Some changes to fire behavior were noted when leather was treated with IFR compounds during tanning. APP_12 exhibited low smoke production rates after ignition compared to unfilled leather, and its TSR (Figure 6c) was strongly reduced versus unfilled leather. This outcome points to the smoke suppressant effects of APP upon the grain side of the leather. For MELA_12, TSR was also reduced, indicating that melamine influenced the smoke production of IFR-tanned leather in the developing fire scenario.

Specific IFR combinations affected the fire properties and the smoke production of leather in fires: APP_6/MELA_6 exhibited a t_{ig} prolonged by 8 s, leading to a 12% reduction in fire growth rate, as FIGRA = max (HRR/t). The interaction of melamine with APP in APP_6/MELA_6 affected the combustion efficiency of the flame, as evidenced by a 15% increase in carbon monoxide yield (COY) to 17.2 × 10 kg kg^{-1}. APP_6/PENTA_6 exhibited a decrease in FIGRA (12% vs unfilled leather) due to lower HRR. Moreover, its peak of heat release rate (PHRR) was reduced by 12% versus unfilled leather. These results point to a strong presence of APP in IFR-tanned leather. Its presence notably affected fire performance. What is more, the results of MELA_6/PENTA_6 displayed a substantial decrease in average specific extinction area (SEA) compared to unfilled leather due to the low smoke production. The SEA decreased by 24% to 69.2 m^2 kg^{-1} (vs 90.7 m^2 kg^{-1} of unfilled leather). These observations point to the key role of melamine in affecting the smoke production of leather in fires. INTUM_6 displayed the most significant impact on fire parameters among INTUM specimens: PHRR was the lowest (175 kW m^{-2}, a decrease of 14%) (Figure 6a), with similar trends for FIGRA, THE, EHC, COY, TSR, and SEA. This result highlights the effectiveness of IFR additives added during the tanning of leather. The fire parameters were clearly reduced for IFR-tanned leather compared to unfilled leather, implying that additives used in the tanning process can influence fire behavior.

https://doi.org/10.1021/acsomega.2c05633
ACS Omega 2022, 7, 44156−44169

Table 2. Key Values from Cone Calorimetry Measurements: Time to Ignition (t_{ig}), Peak of HRR (PHRR), Fire Growth Rate (FIGRA), Total Heat Evolved (THE), Residue Yield, Effective Heat of Combustion (EHC), Carbon Monoxide Yield (COY), and SEA

sample	t_{ig}/s	PHRR/kW m^{-2}	FIGRA/kW m^{-2} s^{-1}	THE/MJ m^{-2}	residue/wt %	EHC/MJ kg^{-1}	TSR/m^2 m^{-2}	COY/10^3 kg kg^{-1}	SEA/m^2 kg^{-1}
leather	34 ± 1	203 ± 4	3.4 ± 0.1	8.8 ± 0.2	26.7 ± 1.4	13.3 ± 0.3	60.0 ± 3.9	15.0 ± 1.0	90.7 ± 4.6
APP_12	30 ± 2	182 ± 6	3.2 ± 0.1	8.1 ± 0.1	27.9 ± 0.1	13.0 ± 0.1	53.1 ± 0.9	16.3 ± 0.1	84.5 ± 1.2
MELA_12	36 ± 1	192 ± 4	3.3 ± 0.1	8.3 ± 0.2	26.7 ± 0.4	12.5 ± 0.1	43.9 ± 2.0	15.5 ± 0.2	62.4 ± 0.9
PENTA_12	36 ± 2	186 ± 3	3.2 ± 0.1	8.4 ± 0.1	23.6 ± 1.0	12.6 ± 0.3	58.2 ± 2.1	16.3 ± 1.2	89.7 ± 4.8
MELA_6/PENTA_6	33 ± 3	189 ± 3	3.3 ± 0.1	8.6 ± 0.5	24.8 ± 0.1	12.8 ± 0.4	41.0 ± 0.3	14.6 ± 0.6	69.2 ± 2.7
APP_6/MELA_6	42 ± 4	192 ± 4	3.0 ± 0.1	9.0 ± 0.2	27.8 ± 0.4	12.0 ± 0.3	49.0 ± 3.4	17.2 ± 1.1	71.0 ± 1.9
APP_6 PENTA_6	37 ± 1	178 ± 5	3.0 ± 0.1	8.2 ± 0.1	27.1 ± 4.9	13.1 ± 0.9	55.1 ± 1.3	16.5 ± 1.7	90.9 ± 2.6
INTUM_3	33 ± 1	182 ± 4	3.2 ± 0.1	8.4 ± 0.1	27.0 ± 1.3	13.1 ± 0.1	55.2 ± 1.5	15.7 ± 0.7	89.0 ± 3.4
INTUM_6	35 ± 2	175 ± 3	3.1 ± 0.1	8.1 ± 0.2	26.2 ± 0.5	12.6 ± 0.3	47.4 ± 0.6	17.1 ± 0.7	82.7 ± 4.1
INTUM_12	38 ± 1	203 ± 3	3.4 ± 0.1	8.8 ± 0.4	26.5 ± 0.9	12.7 ± 0.5	59.5 ± 2.4	15.9 ± 0.8	87.3 ± 3.1

Cone calorimetry measurements highlighted the influence of melamine in smoke production and its cooperative effect with APP in affecting the fire behavior of leather. FR effects of leather with APP and melamine have been studied previously.[30] The interaction of phosphorus with collagen coupled with melamine acting in the gas phase led to increased flame retardancy of the material. A similar mode of action was observed for APP_6/MELA_6 and INTUM_6, which displayed smoke suppression and flame retardancy effects that led to improved fire performance. Particularly, MELA_12, MELA_6/PENTA_6, APP_6/MELA_6, APP_6/PENTA_6, and INTUM_6 showed unique impacts on the smoke production of leather in fires. These specimens were further investigated in smoke density chamber (SDC) measurements to ascertain their impact on the smoke production and toxicity of leather in fire scenarios.

3.4.3. Residue Analysis. Photographs of leather residues after fire tests (Figure 7) showed that leather retained a brittle residue. It displayed characteristics of porous skin on the grain side (Figures 7a, S3a,c) even after fire testing due to carbonaceous residues which were formed during the decomposition of the proteinaceous scaffold. The SEM images of flesh side residues (Figure S3b,d) revealed largely intact leather fibers remaining after fire. Further residue and SEM images are found in the Supporting Information (Figures S3−S9).

IFR leathers exhibited visibly altered surface morphology (Figure 7b−f): MELA_12 (Figure 7b) displayed a coarse, fused surface compared to unfilled leather, while samples containing APP exhibited a smoother, closed surface. Particularly, APP_6/PENTA_6 exhibited an inorganic layer along the surface. A similar structure was visible in Figure 7f for INTUM_6, where the combination of melamine, APP, and pentaerythritol formed an inorganic layer during a fire. This observation points to the following flame retardancy mode of action for IFR-tanned leather: for INTUM_6, a protective layer formed on the grain side during a fire, lowering the PHRR and THE compared to unfilled leather. The layer suppressed smoke production, as evidenced by lower TSR compared to unfilled leather. These effects were most pronounced for INTUM_6 compared to other IFR. Previous investigations on combinations of phosphorus flame retardants and proteinaceous animal products also pointed to enhanced flame retardancy of the material; the amino acids of structural proteins are phosphorylated and enhance the condensed phase activity.[31] Thus, SEM measurements pointed to the fire-retardant effects of IFR compounds added during the tanning of leather. The residues clearly indicate that the IFR compounds were retained during the tanning processes.

3.4.4. Smoke Production. To better understand the impact of IFR-tanned leather on the smoke production and smoke toxicity of leather in fire scenarios, specific specimens were further investigated in SDC measurements, where the specific optical density (D_s) was determined. The D_s and mass optical density (MOD) as functions of time are displayed in Figure 8. Before ignition, all specimens exhibited smoldering behavior. Consequently, D_s rose before t_{ig}. After ignition, the smoke density reached its maximum, followed by a plateau (Figure 8a). The flame spread acted as an external light source, which was detected by the photomultiplier, thereby reducing D_s.

$$\mathrm{MOD} = \frac{0.51\ \mathrm{m}^3}{0.915\ \mathrm{m}} \cdot \frac{D_s}{\Delta m} \quad (1)$$

https://doi.org/10.1021/acsomega.2c05633
ACS Omega 2022, 7, 44156−44169

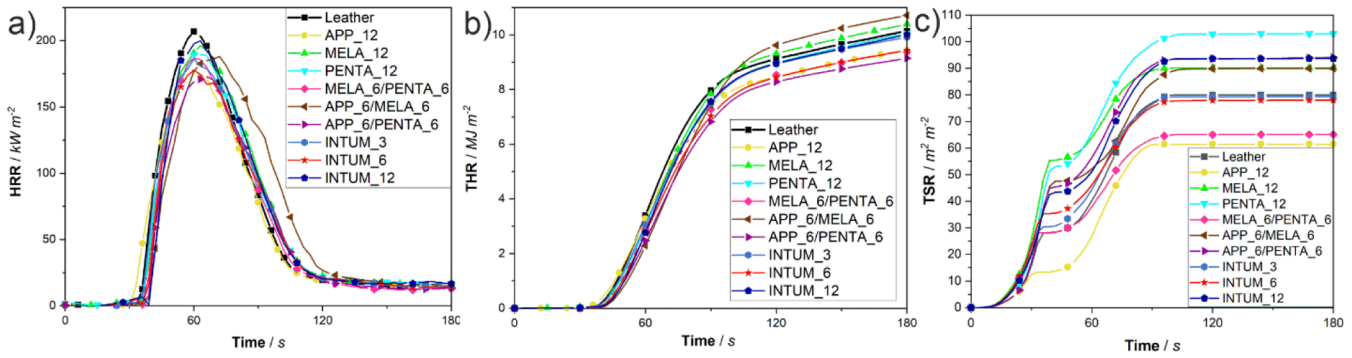

Figure 6. Results from cone calorimetry measurements, displaying (a) heat release rate (HRR), (b) THR, and (c) TSR of unfilled leather and IFR leather samples as functions of time.

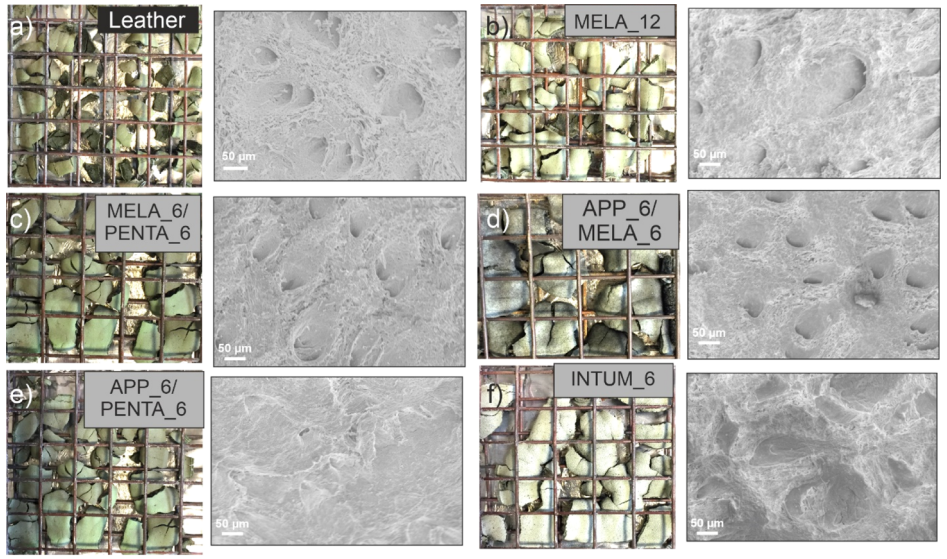

Figure 7. Grain-side residue photographs and SEM images of (IFR) leather samples: (a) leather; (b) MELA_12; (c) MELA_6/PENTA_6; (d) APP_6/MELA_6; (e) APP_6/PENTA_6; (f) INTUM_6.

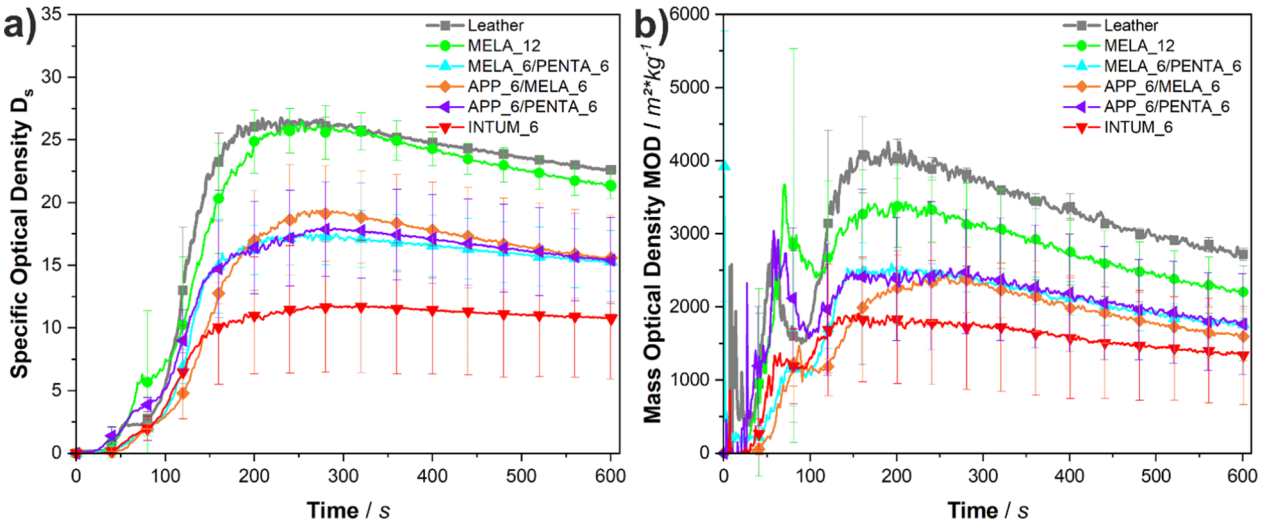

Figure 8. (a) Time-dependent specific optical density and (b) MOD of different (IFR) leather samples.

Equation 1 displays the relationship between MOD, D_s, and the mass loss Δm. After ignition ($t \geq 60$ s), a drop in MOD was observed (Figure 8b). As D_s did not decrease in this period, the reduction of MOD implied that mass loss was the driving force. Moreover, a drop in MOD as compared to the reference value pointed to the formation of a barrier. As barrier effects have a retardant effect on mass loss, the reduction in MOD of INTUM_6 and APP_6/MELA_6 versus unfilled

https://doi.org/10.1021/acsomega.2c05633
ACS Omega 2022, 7, 44156−44169

Table 3. Time of Ignition (t_{ig}), Flaming Burning time (T_{flame}), Maximum of Specific Optical Density ($D_{s,max}$), the Residue Yield, and the Conventional Index of Toxicity after 8 min (CIT_8) *Uncertainty Estimated (See the Supporting Information)

sample	t_{ig}/s	t_{flame}/s	$D_{s,max}$	residue yield/%	CIT_8
leather	58 ± 6	135 ± 2	26.7 ± 0.4	8.0 ± 2.5	0.36 ± 0.01
MELA_12	84 ± 16	133 ± 26	26.5 ± 1.5	10.9 ± 2.2	0.43 ± 0.06
MELA_6/PENTA_6	64 ± 4	125 ± 2	17.5 ± 2.5	10.6 ± 0.9	0.40 ± 0.03
APP_6/MELA_6	78 ± 6	140 ± 5	19.3 ± 4.3	17.4 ± 2.2	0.43 ± 0.01
APP_6/PENTA_6	60 ± 4	147 ± 8	17.9 ± 3.7	15.5 ± 13.9	0.46 ± 0.08
INTUM_6	64 ± 5	144 ± 5	11.7 ± 5.2	11.4 ± 4.2	0.40 ± 0.01

leather was attributed to the formation of a barrier along the grain-side surface. Due to rapid mass loss after ignition, D_s increased drastically because of the emission of gases and particles.

Leather and MELA_12 showed the highest value of $D_{s,max}$ (26.5), while INTUM_6 exhibited the lowest value (11.7). Correspondingly, SEM images of the residues revealed a rough, partly porous surface structure, whereas INTUM_6 exhibited a closed smooth surface. Consequently, the dense layer reduced mass transfer rates, which inhibited gas and particle emission. Producing a closed, stable surface appears to be the most important mechanism to suppress smoke in burning leather. Although the mass loss of INTUM_6 was equal to that of unfilled leather, D_s was significantly reduced. The "high" D_s of MELA_12 was attributed to melamine content; lower content led to lower D_s. The results from TG-FTIR analysis and Py-GC/MS provide supporting evidence that melamine was an effluent in the pyrolytic decomposition of MELA_12 and melamine-containing leather specimens. Furthermore, MELA_12 and APP_6/MELA_6 retarded the time to ignition (t_{ig}) compared to unfilled leather (an increase of 26 and 20 s, respectively) (see Table 3). Moreover, the flaming burning time (t_{flame}) was clearly affected for APP_6/PENTA_6 and INTUM_6, increasing it by 9−12 s, respectively. The prolongation of the burning time and increased residue suggest the formation of a protective layer.

The results from optical density measurements affirm a smoke-suppressing and barrier-forming mode of action for leather tanned with IFR compounds. Particularly, INTUM_6 displayed an impact on $D_{s,max}$ and MOD, signifying that the IFR compounds were integrated into the leather during tanning and retained to impart FR properties onto the material.

To analyze the composition of smoke gases, FTIR measurements were conducted during the burning of samples in the SDC (Figure 9). The smoke toxicity was estimated via the conventional index of toxicity (CIT). A slight increase in the toxicity of IFR leather samples was noted, attributed to the increased production of CO, NO, and HCN (Tables 3 and S4) from incomplete combustion. Although many of these gases are harmful, smoke toxicity increased only slightly. Every (IFR) leather sample fulfilled the optical density and smoke toxicity requirements for use as a seat cover in trains according to the DIN EN 45545 standard, achieving the highest hazard level HL3 (see Table S4).

All samples showed moderate CO emissions during burning (Figure 9a), but after flameout, the CO concentration clearly increased due to thermo-oxidative decomposition. Especially, APP_6/MELA_6 showed high CO concentrations after flameout from the afterglow, and melamine-containing samples saw an increase in CO production. During burning, CO_2 production was higher than CO, but at flameout, the CO_2 concentration increased constantly during the afterglow in all samples.

FTIR experiments revealed that SO_2 gas was emitted at high levels (up to 120 ppm for MELA_12), attributed mainly to the tanning process of leather: During burning, chromium sulfate and sulfinated fatting agents led to the production of SO_2. SO_2 emissions were reduced by 20% for APP_6/PENTA_6 and INTUM_6 compared to unfilled leather, to around 80 ppm. Both materials showed a dense surface morphology in SEM images (Figure 7d,e), providing evidence for protective barriers hindering the decomposition of tanning agents to form SO_2. Ammonia emissions were low, although collagen and melamine were abundant nitrogen sources because NH_3 was oxidized to NO_x. The condensation of melamine to melam or to melem and melon was negligible as there is no significant residue increase attributed to melem or melon.[32] For nitrogen oxides, NO is the main NO_x species emitted. Adding IFR components to leather increased NO production, depending on the APP content. NO_2 emissions rose with increasing melamine content. Furthermore, APP increased the emission of N_2O (Figure 9h). Samples containing APP and melamine produced more N_2O during the afterglow.

After flameout, a rapid increase in HCN was observed, especially for APP_6/MELA_6. As hydrogen cyanide is about 25 times more toxic than carbon monoxide,[33] minimizing its emission is essential to increase safety in fires. Unfilled leather and APP_6/PENTA_6 emitted only small amounts of HCN due to lower nitrogen content compared to samples containing melamine. INTUM_6 produced the same concentration of HCN as MELA_6/PENTA_6 at only 2 wt % melamine content, pointing to changes in smoke gas composition for specific IFR leather composites due to barrier effects and incomplete combustion of the material.

3.5. Proposed Smoke Gas Formation Pathway. During the burning of leather, the hydrolysis of amino acids along the polypeptide chain is accelerated at high thermal energy. Collagen, the primal structural protein of leather, contains repeating segments of glycine, (hydroxy-)proline, and a third amino acid. Thus, the decomposition of glycine contributes to the fire phenomena seen in leather. Py-GC/MS pointed to glycine species in the gas phase, indicating scission reactions (hydrolysis, etc.) and vaporization. Alexandrova et al. showed the kinetic hindrance of decarboxylation of glycine to methylamine and CO_2.[34] Bonifačić et al. illustrated the decomposition of a glycine anion by a radical mechanism, which may be accelerated by phosphates.[35] Thus, a proposed decomposition scheme of glycine (Scheme 1) highlights two decomposition routes: the first entailing self-induced thermal decarboxylation of glycine in unfilled leather (Scheme 1, reaction 1.0) to yield methylamine (product a) and the second route proposing gaseous melamine acting as an activator deprotonating glycine. Afterward, the anion undergoes radical

https://doi.org/10.1021/acsomega.2c05633
ACS Omega 2022, 7, 44156−44169

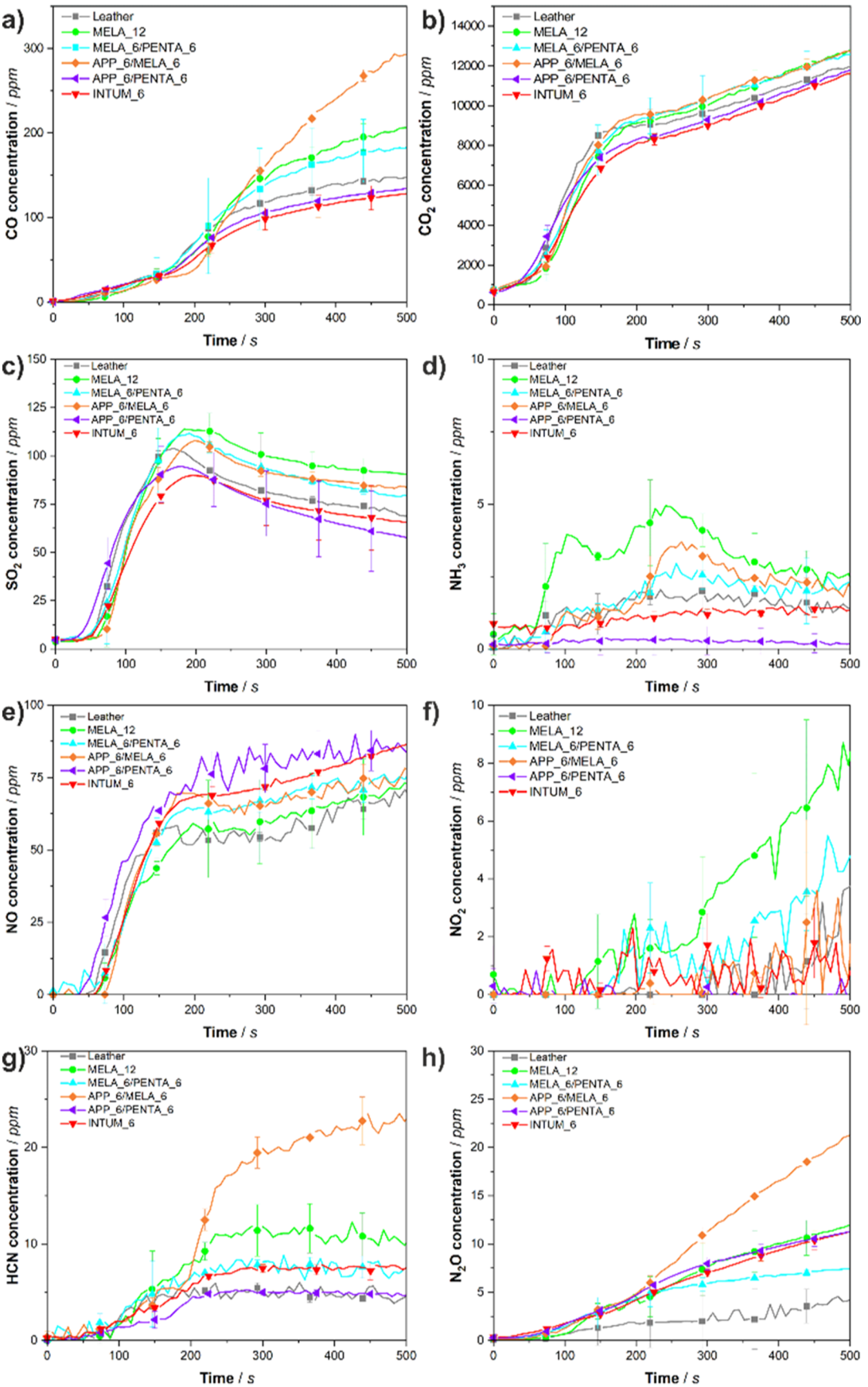

Figure 9. Time-dependent emission of CO (a), CO_2 (b), SO_2 (c), NH_3 (d), NO (e), NO_2 (f), HCN (g), and N_2O (h) of different (FR) leather samples. Measured according to ISO 19702. Samples were treated with 25 kW m^{-2} and additional flaming in the SDC.

https://doi.org/10.1021/acsomega.2c05633
ACS Omega 2022, 7, 44156−44169

Scheme 1. Proposed Decomposition Mechanism of Glycine in the Gas Phase in the SDC

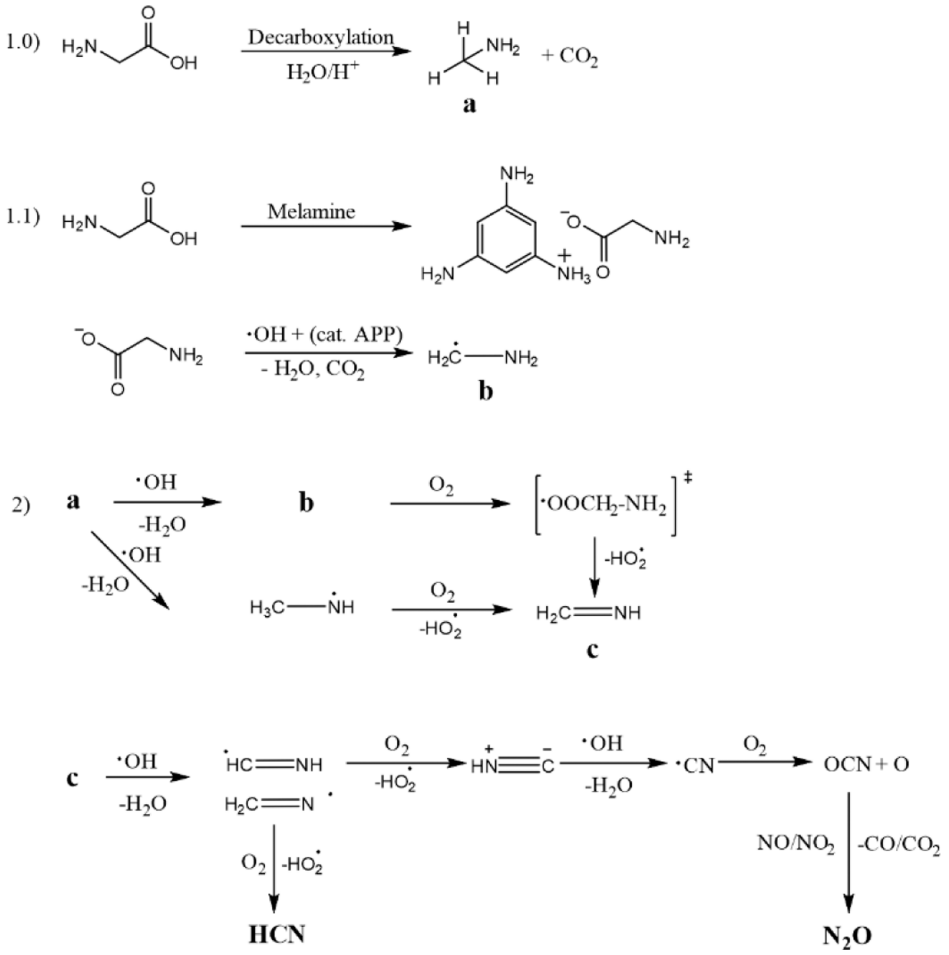

decomposition induced by hydroxy radicals. Methylamine and its radical (product b) decompose according to the radical mechanism described by Schade and Crutzen[36] The two routes merge in the formation of methylene imine (product c).

For unfilled and IFR leather, the two reaction schemes merge in product c, although the paths have different reaction kinetics: the formation of methylamine is kinetically hindered, explaining the low HCN, N_2O, and CO concentrations in unfilled leather compared to IFR samples. Samples containing melamine (MELA_12, MELA_6/PENTA_6, APP_6/MELA_6, and INTUM_6) showed increased CO, HCN, and N_2O formation compared to unfilled leather, providing evidence for the proposed activation (see Scheme 1, 1.1) in the gas phase. APP was an adjuvant to melamine, promoting the formation of HCN and N_2O: after 500 s, APP_6/MELA_6 (6 wt % melamine) produced twice as much HCN as did MELA_12 (12 wt % melamine), whereas INTUM_6 (2 wt % melamine) emitted 25% less HCN than MELA_12. Thus, HCN production increased in the presence of APP due to phosphates, accelerating the formation of product b (Scheme 1, 1.1). As final products, HCN, N_2O, CO, and CO_2 are formed, and NO_2 may be consumed by forming N_2O, thus explaining why mainly NO was observed in the SDC.

4. CONCLUSIONS

The aim of the work was to investigate the potential of intumescent flame retardants used during the leather tanning process in improving flame retardancy and smoke suppression behavior. Moreover, this article sought to investigate precisely which compounds produce which material response in fires. Mechanical tests revealed changes in material properties for specific IFR mixtures, and reaction-to-small-flame tests illustrated improved fire behavior for leathers tanned with IFR compounds. Pyrolysis analysis highlighted melamine's effect in the gas phase and APP's influence on the condensed phase. Forced flaming tests confirmed that INTUM_6 exhibited decreased peak heat release, fire load, and EHC compared to unfilled leather. The SEM images displayed residue formation as a mode of action in fires, and SDC measurements emphasized the interaction of APP and melamine to form smoke-suppressing barriers, further affecting the gas composition of smoke, particularly during afterglow. The incorporation of IFR compounds into the leather during the tanning process signifies a large step in treating leather to improve fire safety. Moreover, the cost-intensive spraying of FRs onto the leather is entirely replaced with a single change in the processing step. The results demonstrate that adding IFR additives during tanning presents a unique, time-, labor-, and cost-effective approach to imparting flame retardancy and smoke suppression to leather.

■ ASSOCIATED CONTENT

Supporting Information

The Supporting Information is available free of charge at https://pubs.acs.org/doi/10.1021/acsomega.2c05633.

https://doi.org/10.1021/acsomega.2c05633
ACS Omega 2022, 7, 44156−44169

Characterization methods; peak identification from Py-GC/MS data; afterglow time of leather samples from reaction-to-small-flame tests; residue photograph and SEM images of unfilled leather; SEM images of IFR specimens at various magnifications; toxicity index (CIT) and optical density ($D_{s,max}$) compared to requirements according to DIN EN 45545-2 R21; and photograph of SDC residues (PDF)

AUTHOR INFORMATION

Corresponding Authors

Guadalupe Sanchez Olivares − *CIATEC A.C., Léon, Gto 37545, Mexico;* orcid.org/0000-0003-0633-8398; Email: gsanchez@ciatec.mx

Bernhard Schartel − *Bundesanstalt für Materialforschung und -prüfung (BAM), 12205 Berlin, Germany;* orcid.org/0000-0001-5726-9754; Email: bernhard.schartel@bam.de

Authors

Alexander Battig − *Bundesanstalt für Materialforschung und -prüfung (BAM), 12205 Berlin, Germany;* orcid.org/0000-0002-9461-1368

Sebastian M. Goller − *Bundesanstalt für Materialforschung und -prüfung (BAM), 12205 Berlin, Germany*

Daniel Rockel − *Bundesanstalt für Materialforschung und -prüfung (BAM), 12205 Berlin, Germany*

Victor Ramírez González − *CIATEC A.C., Léon, Gto 37545, Mexico*

Complete contact information is available at: https://pubs.acs.org/10.1021/acsomega.2c05633

Author Contributions

The manuscript was written with contributions from all authors. All authors have given approval to the final version of the manuscript.

Funding

This research did not receive any specific financial support.

Notes

The authors declare no competing financial interest.

ACKNOWLEDGMENTS

The authors thank Yin Yam Chan for her assistance with SEM measurements and Patrick Klack for his assistance with TGA and the cone calorimeter.

ABBREVIATIONS

FR, flame retardant; IFR, intumescent flame retardant; APP, ammonium polyphosphate; MELA, melamine; PENTA, pentaerythritol; TGA, thermogravimetric analysis; HRR, heat release rate; THR, total heat release; TSR, total smoke release; FIGRA, fire growth rate; THE, total heat evolved; EHC, effective heat of combustion; COY, carbon monoxide yield; SEA, specific extinction area; SDC, smoke density chamber; MOD, mass optical density

REFERENCES

(1) Pringle, T.; Barwood, M.; Rahimifard, S. The Challenges in Achieving a Circular Economy within Leather Recycling. *Procedia CIRP* **2016**, *48*, 544−549.

(2) (a) Pradeep, S.; Sathish, M.; Sreeram, K. J.; Rao, J. R. Melamine-Based Polymeric Crosslinker for Cleaner Leather Production. *ACS Omega* **2021**, *6*, 12965−12976. (b) Sivakumar, V. Towards environmental protection and process safety in leather processing - A comprehensive analysis and review. *Process Saf. Environ. Prot.* **2022**, *163*, 703−726. (c) Popiolski, A. S.; Dallago, R. M.; Steffens, J.; Mignoni, M. L.; Venquiaruto, L. D.; Santos, D.; Duarte, F. A. Ultrasound-Assisted Extraction of Cr from Residual Tannery Leather: Feasibility of Ethylenediaminetetraacetic Acid as the Extraction Solution. *ACS Omega* **2018**, *3*, 16074−16080.

(3) Makovická Osvaldová, L.; Marková, I.; Vandlíčková, M.; Gašpercová, S.; Titko, M. Fire Characteristics of Upholstery Materials in Seats. *Int. J. Environ. Res. Publ. Health* **2020**, *17*, 3341.

(4) Donmez, K.; Kallenberger, W. E. FLAME RESISTANCE OF LEATHER. *J. Am. Leather Chem. Assoc.* **1992**, *87*, 1−19. Huang, Z.; Li, L. X.; Wang, Y. H.; Lin, Y. Z.; Chen, W. Y. Performance of flame retardants on leather. *J. Soc. Leather Technol. Chem.* **2005**, *89*, 225−231.

(5) Bacardit, A.; Casas, C.; Bou, J.; i Otero, L. O. Development of Nanocomposites with Flame Retardant Effect for Leather and Fabric. *J. Soc. Leather Technol. Chem.* **2019**, *103*, 202−207.

(6) Duan, B.; Wang, Q.; Wang, X.; Li, Y.; Zhang, M.; Diao, S. Flame retardance of leather with flame retardant added in retanning process. *Results Phys.* **2019**, *15*, 102717. Chen, Y.; Fan, H.; Shi, B. Nanotechnologies for leather manufacturing: A review. *J. Am. Leather Chem. Assoc.* **2011**, *106*, 260−273. Mohamed, O. A.; Abdel-Mohdy, F. Preparation of flame-retardant leather pretreated with pyrovatex CP. *J. Appl. Polym. Sci.* **2006**, *99*, 2039−2043. Ying, G.; Wuyong, C.; Jiping, C.; Haibin, G. Influence of finishing on the flammability of leather. *J. Soc. Leather Technol. Chem.* **2007**, *91*, 208−211. Wang, Y.; Zheng, M.; Liu, X.; Yue, O.; Wang, X.; Jiang, H. Advanced collagen nanofibers-based functional bio-composites for high-value utilization of leather: A review. *J. Sci.: Adv. Mater. Devices* **2021**, *6*, 153−166.

(7) Lyu, B.; Kou, M.; Gao, D.; Luo, K.; Ma, J.; Lin, Y. Flame retardancy of carboxylated polyhedral oligosilsesquioxane modified layered double hydroxide in the process of leather fatliquoring. *J. Appl. Polym. Sci.* **2022**, *139*, No. e52468.

(8) Jiang, Y.; Li, J.; Li, B.; Liu, H.; Li, Z.; Li, L. Study on a novel multifunctional nanocomposite as flame retardant of leather. *Polym. Degrad. Stab.* **2015**, *115*, 110−116.

(9) Sanchez-Olivares, G.; Sanchez-Solis, A.; Calderas, F.; Medina-Torres, L.; Manero, O.; Di Blasio, A.; Alongi, J. Sodium montmorillonite effect on the morphology, thermal, flame retardant and mechanical properties of semi-finished leather. *Appl. Clay Sci.* **2014**, *102*, 254−260.

(10) Lyu, B.; Luo, K.; Gao, D.; Wang, Y.; Ma, J. Synergistic effect of layered double hydroxide and montmorillonite: Towards super-efficient fireproofing of leather. *Appl. Clay Sci.* **2021**, *212*, 106215.

(11) He, Y.; Zhang, Z.; Fan, H.; Yan, J. Graphene Oxide Grafted Maleic Anhydride Vinyl Acetate Co-polymer and its Enhancement of Flame Retardance and UV-resistance of Retanned Leather. *J. Am. Leather Chem. Assoc.* **2019**, *114*, 216.

(12) Yang, X.; Li, Y.; Yang, M.; Dang, X.; Cao, S. High Performance Leather based on in Situ Formation of Reduced Graphene Oxide in Chrome Tanning. *J. Am. Leather Chem. Assoc.* **2022**, *117*, 206−211.

(13) Lyu, B.; Luo, K.; Gao, D.; Wang, Y.; Ma, J. Modified layered double hydroxide/zanthoxylum bungeanum seed oil composites to improve the flame retardant of leather. *Polym. Degrad. Stab.* **2021**, *183*, 109430.

(14) Lyu, B.; Luo, K.; Wang, Y.; Gao, D.; Ma, J. Sodium alginate oxide assembly layered double hydroxide and its structure-activity relationship to anti-fogging properties and flame retardancy of leather. *Appl. Clay Sci.* **2020**, *190*, 105559. Lyu, B.; Gao, J.; Ma, J.; Gao, D.; Wang, H.; Han, X. Nanocomposite based on erucic acid modified montmorillonite/sulfited rapeseed oil: Preparation and application in leather. *Appl. Clay Sci.* **2016**, *121−122*, 36−45. Lyu, B.; Wang, Y.-F.; Gao, D.-g.; Ma, J.-z.; Li, Y. Intercalation of modified zanthoxylum bungeanum maxin seed oil/ stearate in layered double hydroxide: Toward flame retardant nanocomposites. *J. Environ. Manage.* **2019**, *238*, 235−242.

(15) Zhang, S.; Horrocks, R. Substantive intumescent flame retardants for functional fibrous polymers. *J. Mater. Sci.* **2003**, *38*, 2195−2198.
(16) Li, B.; Li, J.; Li, L.; Jiang, X.; Li, Z. Synthesis and Application of Novel Functional Material as Leather Flame Retardant. *J. Am. Leather Chem. Assoc.* **2014**, *109*, 239−245.
(17) Xu, W.; Li, J.; Liu, F.; Jiang, Y.; Li, Z.; Li, L. Study on the thermal decomposition kinetics and flammability performance of a flame-retardant leather. *J. Therm. Anal. Calorim.* **2017**, *128*, 1107−1116.
(18) Price, D.; Liu, Y.; Milnes, G. J.; Hull, R.; Kandola, B. K.; Horrocks, A. R. An investigation into the mechanism of flame retardancy and smoke suppression by melamine in flexible polyurethane foam. *Fire Mater.* **2002**, *26*, 201−206.
(19) Covington, A. D.; Wise, W. R.Tanning Chemistry. *The Science of Leather*, 2nd ed.; Royal Society of Chemistry, 2019.
(20) Wachsmann, H. M.Retannage. In *Leather Technologists Pocket Book*; Leafe, M. K., Ed.; Society of Leather Technologists and Chemists, 1999; pp 85−98. Schubert, A.The manufacture of leather from calfskin. In *The Chemistry and Technology of Leather*, O'Flaherty, F., Roddy, W. T., Lollar, R. M., Eds.; Vol. 3; Robert E. Krieger Publishing Company, 1978; pp 205−214.
(21) Liu, C.-K.; Latona, N. P.; DiMaio, G. L.; Cooke, P. H. Viscoelasticity studies for a fibrous collagen material: chrome-free leather. *J. Mater. Sci.* **2007**, *42*, 8509−8516. Wright, D. M.; Attenburrow, G. E. The set and mechanical behaviour of partially processed leather dried under strain. *J. Mater. Sci.* **2000**, *35*, 1353−1357.
(22) Bugby, A.Microscopy. In *Leather Technologists Poket Book*; Leafe, M. K., Ed.; Society of Leather Technologists and Chemists, 1999; pp 325−332.
(23) Ward, A. G. The mechanical properties of leather. *Rheol. Acta* **1974**, *13*, 103−112.
(24) Donmez, K.; Kallenberger, W. An overview of testing of leather for flame/glow retardance. *J. Am. Leather Chem. Assoc.* **1991**, *86*, 93−106.
(25) Kunze, R.; Schartel, B.; Bartholmai, M.; Neubert, D.; Schriever, R. TG-MS and TG-FTIR applied for an unambiguous thermal analysis of intumescent coatings. *J. Therm. Anal. Calorim.* **2002**, *70*, 897−909.
(26) Costa, L.; Camino, G.; Luda di Cortemiglia, M. P.Mechanism of thermal degradation of fire-retardant melamine salts. In *Fire and Polymers Hazards Identification and Prevention*; Nelson, G. L., Ed.; ACS Publications, 1990; pp 211−238.
(27) Daus, L.-H.; Schartel, B.; Wachtendorf, V.; Mangelsdorf, R.; Korzen, M. A chain is no stronger than its weakest link: Weathering resistance of water-based intumescent coatings for steel applications. *J. Fire Sci.* **2021**, *39*, 72−102.
(28) Bourbigot, S.; Duquesne, S.Intumescence-Based Fire Retardants. In *Fire Retardancy of Polymeric Materials*, 2nd ed.; Wilkie, C. A., Morgan, A. B., Eds.; CRC Press, 2009; pp 129−162. Gültek, A. S.; Celik, C.; Acikel, S. M. Investigation of Flame Retardant Effects of Resins on the Flammability of Leather. *Text. Apparel* **2021**, *31*, 3−9.
(29) Schartel, B.; Hull, T. Development of fire-retarded materials-Interpretation of cone calorimeter data. *Fire Mater.* **2007**, *31*, 327−354.
(30) Battig, A.; Sanchez-Olivares, G.; Rockel, D.; Maldonado-Santoyo, M.; Schartel, B. Waste not, want not: The use of leather waste in flame retarded EVA. *Mater. Des.* **2021**, *210*, 110100.
(31) Battig, A.; González, K. I. G.; Schartel, B. Valorizing "non-vegan" bio-fillers: Synergists for phosphorus flame retardants in epoxy resins. *Polym. Degrad. Stab.* **2022**, *198*, 109875. Gleuwitz, F. R.; Battig, A.; Schartel, B. Tenebrio molitor Beetle as a "Nonvegan" Adjuvant to Flame Retardants in Tannic Acid-Based Epoxy Thermosets. *ACS Sustainable Chem. Eng.* **2022**, *10*, 6313−6324.
(32) Levchik, S.; Balabanovich, A.; Ivashkevich, O.; Gaponik, P.; Costa, L. Thermal decomposition of tetrazole-containing polymers. V. Poly-1-vinyl-5-aminotetrazole. *Polym. Degrad. Stabil.* **1995**, *47*, 333−338.
(33) Stec, A. A.; Hull, T. R.*Fire Toxicity*; Elsevier, 2010.
(34) Alexandrova, A. N.; Jorgensen, W. L. On the mechanism and rate of spontaneous decomposition of amino acids. *J. Phys. Chem. B* **2011**, *115*, 13624−13632.
(35) Bonifačić, M.; Štefanić, I.; Hug, G. L.; Armstrong, D. A.; Asmus, K.-D. Glycine decarboxylation: the free radical mechanism. *J. Am. Chem. Soc.* **1998**, *120*, 9930−9940.
(36) Schade, G. W.; Crutzen, P. J. Emission of aliphatic amines from animal husbandry and their reactions: Potential source of N2O and HCN. *J. Atmos. Chem.* **1995**, *22*, 319−346.

https://doi.org/10.1021/acsomega.2c05633
ACS Omega 2022, 7, 44156−44169